

Magnetically-Excited Flexural Plate Wave Device **RECEIVED**

M. A. Butler, S. J. Martin, J. J. Spates, and M-A Mitchell
Sandia National Laboratories, Albuquerque, NM 87185-1425

MAY 08 1997

OSTI

SUMMARY

Novel devices have been designed, fabricated, and tested that use the Lorentz force to excite flexural plate waves in a silicon nitride membrane. Single and dual port devices have been fabricated and the excitation spectra measured. Eigenmodes of the membrane are excited in this resonant device and non-linear effects, due to amplitude stiffening of the membrane, are observed. The effects of temperature and ambient gas on resonant frequency and Q have been explored. These devices have the advantage of material compatibility with silicon process technology and are capable of operating at very high temperatures.

Keywords: magnetic excitation, flexural plate wave, resonant sensor.

INTRODUCTION

Conventional flexural plate wave (FPW) devices use interdigitated electrodes patterned on a piezoelectric film to excite and detect acoustic waves in a thin membrane [1]. Unfortunately, the piezoelectric materials are difficult to process and are typically incompatible with conventional silicon process technology. Furthermore, piezoelectric excitation limits the forces that can be applied to the membrane due to dielectric breakdown. To overcome some of these limitations, a new type of FPW resonator has been constructed that utilizes a meander-line transducer in a static magnetic field to excite acoustic waves in a membrane via Lorentz forces [2]. Such a device is shown in figure 1.

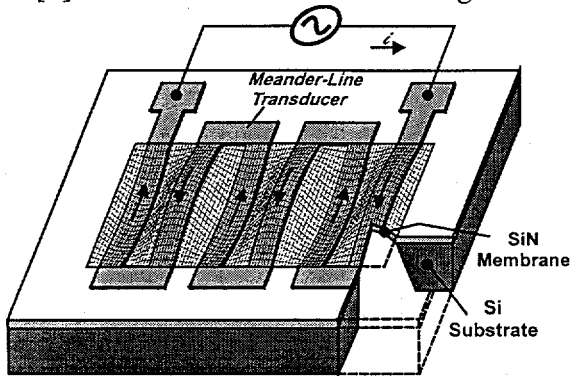


Fig. 1 Drawing of a single port, magnetically excited, FPW resonator. The nitride is about 2 μm thick and the meanderline conductor is 0.5 μm thick Au over Cr.

The device is fabricated using conventional lithographic methods to pattern the transducer and define the membrane size. Bulk micromachining is then used to release the membrane. The meander-line transducer (MLT) is located appropriately to excite eigenmodes of the membrane. This is a resonant device can have Q values in vacuum as high as 10,000.

THEORY

Application of an AC current at a frequency $f=v_0/\lambda$ (v_0 is the FPW phase velocity and λ is the MLT periodicity) to the MLT in figure 1 with an in-plane, static magnetic field present excites standing waves in the membrane. The partial differential equation describing surface-normal displacement u is:

$$D\nabla^4 u - Th\nabla^2 u + Z_a \dot{u} + \rho_s \ddot{u} = \vec{F} \quad (1)$$

where D , T , h , and ρ_s are the membrane bending moment, in-plane stress, thickness, and areal mass density, respectively; Z_a is a mechanical impedance arising from contacting fluid (gas or liquid); \vec{F} is the surface-normal Lorentz force $J \times B$ where B is the applied magnetic field and J the current density. Internal damping of the membrane can be accounted for by using a complex Young's modulus in calculating D . Solution of this equation leads to the eigenmodes of the membrane with resonances occurring at the following frequencies [3]

$$\omega = k \left(\frac{Dk^2 + Th}{\rho_s} \right)^{1/2} \quad (2)$$

where k is the wavenumber. For the devices considered here, the membrane tension is a major contributor to the resonant frequency. Thus, variations in residual stress in the low stress nitride membrane will cause variations in the resonant frequency. Similarly, large amplitudes of oscillation, resulting from the large driving forces and large Q, effectively stretch the membrane and raise its average stress. This "amplitude-stiffening" effect, observed in other microstructures [4], will also cause significant frequency shifts.

Efficient excitation of the eigenmodes by the MLT depends on magnetic field strength, location of the current lines relative to displacement maxima and the number of MLT periods, N . The impedance response of a single-port device is given by:

MASTER

DISTRIBUTION OF THIS DOCUMENT IS UNLIMITED

W

DISCLAIMER

This report was prepared as an account of work sponsored by an agency of the United States Government. Neither the United States Government nor any agency thereof, nor any of their employees, makes any warranty, express or implied, or assumes any legal liability or responsibility for the accuracy, completeness, or usefulness of any information, apparatus, product, or process disclosed, or represents that its use would not infringe privately owned rights. Reference herein to any specific commercial product, process, or service by trade name, trademark, manufacturer, or otherwise does not necessarily constitute or imply its endorsement, recommendation, or favoring by the United States Government or any agency thereof. The views and opinions of authors expressed herein do not necessarily state or reflect those of the United States Government or any agency thereof.

DISCLAIMER

**Portions of this document may be illegible
in electronic image products. Images are
produced from the best available original
document.**

$$Z(\omega) = R_0 + \frac{c_2 w B^2 N}{\lambda \left(Z_a + j\omega \rho_s h + \frac{Thk^2}{j\omega} + \frac{Dk^4}{j\omega} \right)} \quad (3)$$

where R_0 is the DC resistance of the MLT, w is the width of the membrane, and λ is the wavelength.

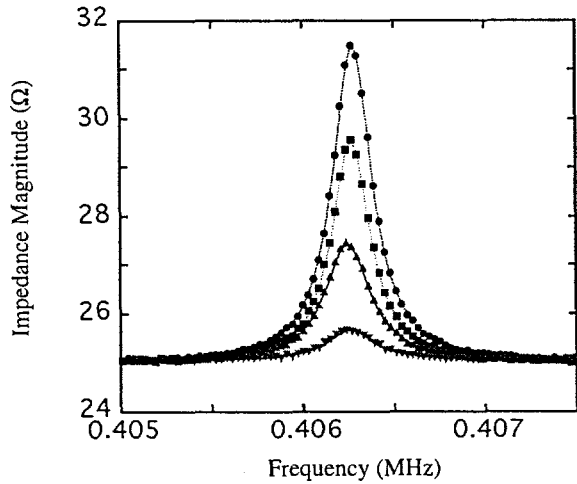


Fig. 2 Impedance response of a single-port Mag-FPW resonator in air for magnetic field strengths of 7.78, 6.45, 4.69, and 2.38 kG.

EXPERIMENTAL RESULTS

The devices were fabricated using conventional lithographic processes on 200 μm -thick (100) silicon wafers coated on both sides with 2 μm of low stress nitride. The MLT is 0.5 μm gold over a thin Cr adhesive layer. Typical DC resistance is 25 Ohms. The impedance response of a single-port device with a 2.2 x 3.4 mm membrane is shown in figure 2. The wavelength of the standing wave is

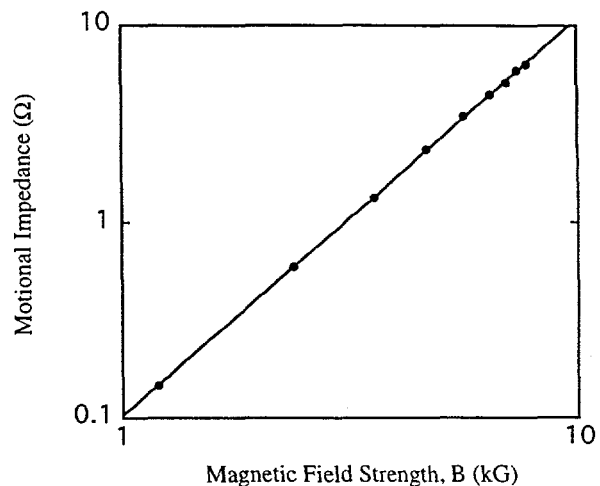


Fig. 3 Motional impedance versus magnetic field strength. The straight line is a power law fit with a slope of 2.02

320 μm . Coupling efficiency, and thus motional impedance, varies quadratically with magnetic field strength as expected (Fig. 3). By examining several devices with different wavelengths, the dispersion curve (ω vs. k) can be plotted (Fig. 4). Fitting Eq. 2 to this data determines the membrane bending moment D and in-plane stress T (ρ_s is calculated). Both are reasonable numbers for these materials and processes.

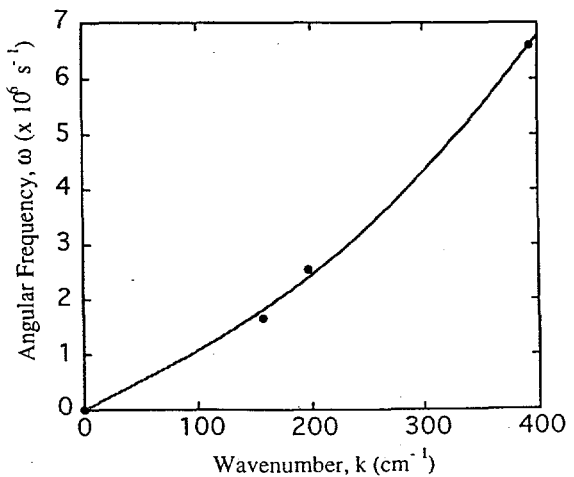


Fig. 4 Dispersion curve for the FPW modes in a 2 μm -thick silicon nitride membrane. The line is a fit of Eq. 2 to the data which determines bending moment, $D=1.84$ dyne-cm. and in-plane stress, $T=6.1 \times 10^8$ dynes/cm 2 .

For these devices membrane stress is an important contribution to the resonant frequency (Eq. 2). Thus environmental factors that can influence the membrane stress will result in shifts in frequency, e.g. temperature, pressure, etc. Since the bending moment is less sensitive to environmental factors, use of this device for these sensing applications is best achieved by maximizing the stress contribution relative to bending moment.

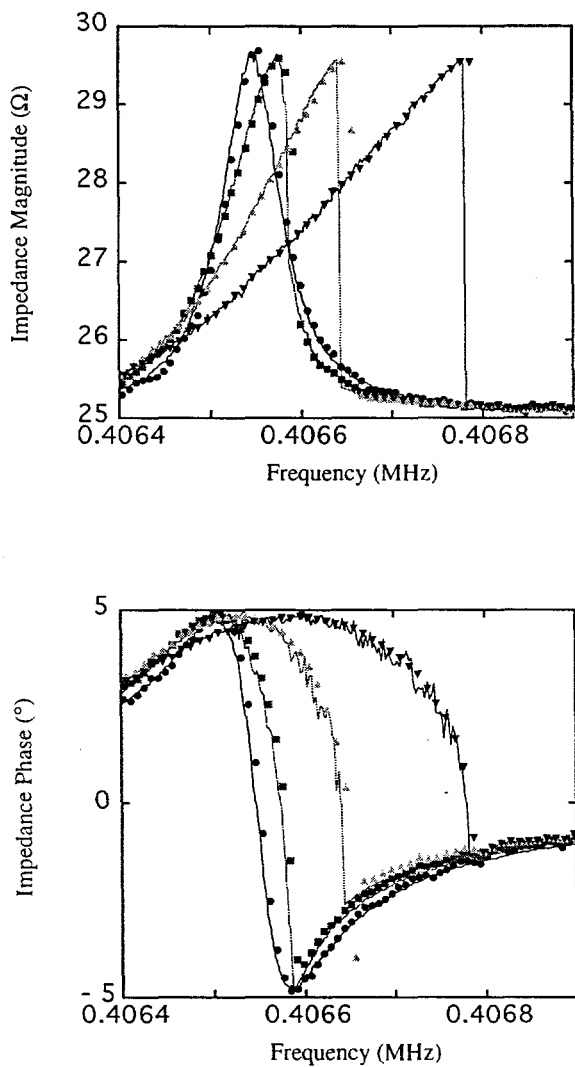


Fig. 5 The impedance spectrum measured with increasing frequency for power levels of: -43, -31, -27, and -24 dBm in vacuum. The lines are model calculations.

Because of the strong sensitivity of the resonant frequency to stress and the resonant nature of the device, amplitude-induced stiffening of the membrane can result in frequency pulling effects. As a standing wave is excited in the membrane, the membrane is stretched and the average tension increases. This shifts the resonance to higher

frequencies. Eventually the excitation frequency exceeds the resonant frequency, amplitude decreases, and resonant frequency drops. This results in a discontinuity in impedance at higher input powers. This behavior is shown in Fig. 5. Note that very small input power levels are required for amplitude stiffening to become important. This is because of the large Q_s of these devices. At higher power levels the impedance becomes a triple-valued function and sharp transitions occur between states.

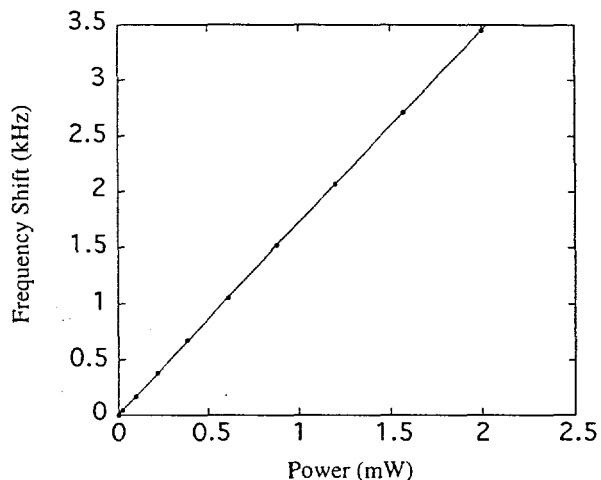


Fig. 6 Magnitude of the frequency decrease as DC power input is increased. The slope of the line is 1.7217 kHz/mW.

Many other factors such as differential pressure, strain, and temperature change the stress in the membrane and the resulting frequency shift can be used for sensing applications. An interesting example is shown in Fig. 6. Here the MLT has DC current simultaneously applied with the RF excitation current. The DC current heats the membrane with respect to the silicon frame which lowers the tension in the membrane and decreases the resonant frequency. This effect has the opposite sign from the amplitude-stiffening effect. Thus the resonance can be tuned by application of a DC current. Fig. 6 shows the frequency shift versus applied DC power. The resonance has been tuned over a range of 20 kHz.

The ambient gas in which the device is operated also has an effect on the resonant frequency. For these devices the phase velocity of the FPW is less than the sound velocity in the gas. Consequently, the membrane does not radiate sound, but generates an evanescent field that entrains the gas near the membrane surface. This provides additional mass loading on the membrane and decreases the

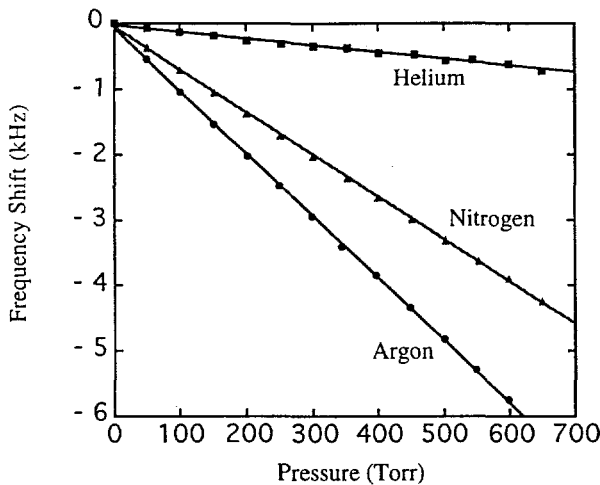


Fig. 7 Frequency shift of the membrane resonance with pressure for different gases.

resonant frequency. A simple model for this loading by the entrained gas gives:

$$\Delta f = \frac{-f N_s \rho}{2k \rho_s \sqrt{1 - \left(\frac{v}{c}\right)^2}} \quad (4)$$

where N_s is the number of membrane sides contacted, ρ is the gas density, f is the resonant frequency, v is the phase velocity of the FPW and c is the velocity of sound in the gas. The expected linear dependence of frequency shift on gas pressure is shown in Fig. 7. The difference between gases is due to their different densities. The gases also have an effect on the Q of the resonance. The standing waves in the membrane generate alternating high and low pressure regions at the membrane surface. This results in lateral flow of the gas across the membrane surface and damping of the resonance due to the viscosity of the gas [5]. A simple equivalent circuit model for this effect gives:

$$\frac{1}{R_2} = \frac{N}{1 - \left(\frac{v}{c}\right)^2} \sqrt{\frac{2\pi f \rho \eta}{2}} \quad (5)$$

where η is the gas viscosity and R_2 is a resistance in the equivalent-circuit model. The expected square-root dependence on pressure is illustrated in Fig. 8. The variation between gases follows the expected square-root of density-viscosity product. These interactions with the gas phase provide an additional mechanism for sensing applications.

SUMMARY

This paper describes a new device, the magnetically-excited flexural plate wave resonator,

and some of its characteristics and the phenomena that are observed with it. We believe it has great potential for sensing applications because of its sensitivity to membrane tension and its resonant nature. It also offers greater displacement amplitudes for pumping applications.

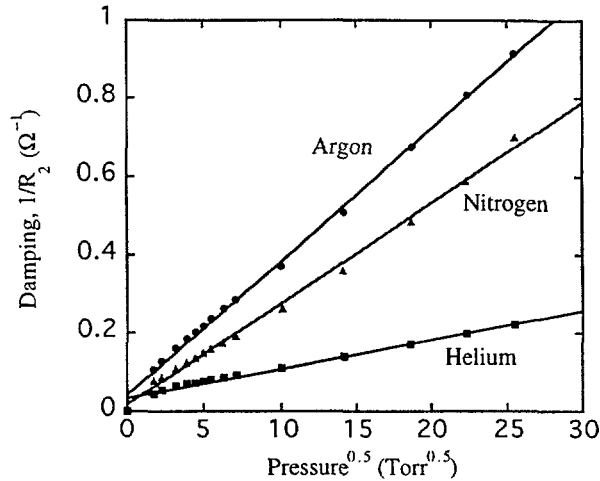


Fig. 8 Damping of the membrane resonance vs. pressure for different gases.

ACKNOWLEDGMENTS

Low stress nitride-coated wafers were kindly provided by Professor T. Kenny of Stanford University. The authors would like to acknowledge helpful discussion with K. Schubert, M. Scott, and G. Frye. This work was supported by the United States Department of Energy under Contract DE-AC04-94AL85000. Sandia is a multi-program laboratory operated by Sandia Corporation, a Lockheed Martin Company, for the United States Department of Energy.

REFERENCES

- [1] S. W. Wenzel and R. M. White, *IEEE Trans. Electron Devices*, ED-35, 735 (1988).
- [2] S. J. Martin, G. C. Frye, J. J. Spates, and M. A. Butler, *IEEE Ultrasonic Sympos. Proc.* (IEEE, New York, 1996) 423-434.
- [3] L. D. Landau and E. M. Lifshitz, *Theory of Elasticity*, 3rd Edition (Pergamon Press, New York, 1986) Ch. 2 & 3.
- [4] T. E. Shirley and S. D. Senturia, "Frequency-Pulling Effects in Amplitude-Stiffened Resonant Sensors," *TRANSDUCERS '93*, 458-461.
- [5] S. W. Wenzel, *Applications of Ultrasonic Lamb Waves*, Ph.D. thesis, Univ. Calif., Berkeley (1992).